Space Charge Simulations of Photoemission Using the Differential Algebra–based Multiple-Level Fast Multipole Algorithm

H. Zhang[1], Z. Tao[2], C.-Y. Ruan[2], M. Berz[2]
[1]Thomas Jefferson National Accelerator Facility, Virginia, USA
[2]Michigan State University, Michigan, USA

Abstract

A grid-free algorithm based on the multiple-level fast multipole algorithm and differential algebra (DA) has been developed to calculate the electrostatic field of an ensemble of charged particles and its high-order derivatives. The efficiency of the algorithm scales linearly with the number of particles for any arbitrary distribution. The algorithm is parallelized to further improve its efficiency. Simulation results on the photoemission process using this algorithm are presented.

Keywords: Space charge effect, fast multipole method, differential algebra (DA), photoemission

1. INTRODUCTION

Collective effects have become more and more important with the need for beams of higher and higher intensity. Numerical simulation is a very useful tool for the study of collective effects, and it is inevitable when the collective effect is strong and highly nonlinear. A new algorithm was developed to calculate the electrostatic field between charged particles. The algorithm combines the multiple level fast multipole algorithm (MLFMA) with differential algebraic (DA) tools (Berz, 1999). The MLFMA has an efficiency of $O(n)$ for n charged particles. Furthermore, it is grid-free; hence, any arbitrary charge distribution can be treated in a natural way. Using DA, we considerably simplify the mathematics, represent the potential as Taylor expansions in the Cartesian coordinates, and calculate not only the field but also its high-order derivatives.

1.1 The Strategy of the Multiple-Level Fast Multipole Algorithm (MLFMA)

In order to evaluate the electrostatic field due to an arbitrary distribution of charges, we divide the charges into groups and evaluate the interactions between the groups far enough away by multipole expansions, and calculate

the interactions between nearby particles directly. The domain containing charged particles is divided into boxes of different sizes according to the charge density in order to keep a roughly equal amount of particles inside each box.

The relation between boxes can be represented as a hierarchical tree. Small boxes generated by splitting a large box are called the *child boxes* of the large box, and the large box is called the *parent box* of the small ones. The boxes that have no child boxes are called *childless boxes*. If the distance between box A and box B is larger than the side length of A, then we can represent the contribution from the charges inside A to the potential in B by a multipole expansion. Also, we can represent the contribution from the charges inside B to the potential inside A by a local expansion.

For a childless box, the multipole expansion is calculated from the charges inside, while for a parent box, the multipole expansion is calculated from the multipole expansions of its child boxes. The local expansion can be calculated from the charges inside a childless box that is far enough away, or from the multipole expansion of a parent box that is far enough away. Child boxes also inherit the local expansions from their parent boxes. The general strategy is to calculate the multipole expansions for all the boxes from the finest level to the coarsest level going upward, and then calculate the local expansions for all the boxes from the coarsest level to the finest level going downward. Once the expansions in all the boxes are calculated, the field on each particle can be calculated separately by two parts. The part due to the particles nearby is calculated using the Coulomb formula directly, while the field due to the particles far away is calculated from the multipole expansions, the local expansions, or both. A detailed description of the MLFMA can be found in reference (Carrier et al., 1988).

1.2 Differential Algebras and COSY INFINITY

In the vector space of the infinitely differentiable functions $C^\infty(R^\nu)$, we define an equivalence relation "$=_p$" between two functions $a, b \in C^\infty(R^\nu)$ via $a =_p b$ if $a(0) = b(0)$ and if all the partial derivatives of a and b at 0 agree up to the order p. Note that the point 0 is selected for convenience, and any other point could be chosen as well. The set of all b that satisfies $b =_p a$ is called the *equivalence class* of a, which is denoted by $[a]_p$. We denote all the equivalence classes with respect to $=_p$ on $C^\infty(R^\nu)$ as ${}_pD_\nu$. The addition, scalar multiplication, multiplication, and the derivation operator ∂_ν can be defined on ${}_pD_\nu$ as

$$[a]_p + [b]_p := [a+b]_p, \quad c \cdot [a]_p := [c \cdot a]_p,$$
$$[a]_p \cdot [b]_p := [a \cdot b]_p, \quad \partial_v [a]_p := [\partial a / \partial x_v]_{p-1},$$

where x_v is the vth variable of the function a, and the operator ∂_v satisfies $\partial_v([a] \cdot [b]) = [a] \cdot (\partial_v[b]) + (\partial_v[a]) \cdot [b]$. Hence ${}_pD_v$ is a differential algebra (DA) (Berz, 1999). There are v special classes $d_v = [x_v]$, whose elements are all infinitely small. If a function a in ${}_pD_v$ has all the derivatives $c_{J_1,\ldots,J_v} = \partial^{J_1+\cdots+J_v} a / \partial x_1^{J_1} \cdot \cdots \cdot \partial x_v^{J_v}$, and then $[a]$ can be written as $[a] = \sum c_{J_1,\ldots,J_v} \cdot d_1^{J_1} \cdot \cdots \cdot d_v^{J_v}$. Thus, $d_1^{J_1} \cdot \cdots \cdot d_v^{J_v}$ is a basis of the vector space of ${}_pD_v$.

COSY INFINITY (Berz & Makino, 2013) is a program developed for high-performance modern scientific computing, which supports DA as an advanced data type. By evaluating a function f in DA data type in COSY, one can get its Taylor expansion f_T, represented by a DA vector, up to an arbitrary predetermined order p automatically. If we consider two functions $f, g \in {}_pD_v$ which can also be viewed as two maps M_f and M_g, the function $f(g)$—i.e., the composition of the two maps $M_f \circ M_g$—can be easily calculated by the command POLVAL in COSY (Berz & Makino, 2013). For more details about DA, refer to Berz (1999).

2. EXPANSIONS IN THE DA FRAMEWORK

Here, we present a summary of the fast multipole method in the DA framework. For full details, we refer to Zhang (2013) and Zhang and Berz (2011).

2.1 The Far Multipole Expansion from the Charges

Suppose that n particles with charge q_i located at $\vec{r}_i(x_i, y_i, z_i)$, with $r_i < a$, then the electrostatic potential at a point $\vec{r}\,(x, y, z)$, with $r > a$ expressed as

$$\phi = \sum_{i=1}^{n} \frac{q_i}{|\vec{r}_i - \vec{r}\,|} = d \cdot \overline{\phi}_{\mathrm{M}}, \tag{1}$$

where

$$\overline{\phi}_{\mathrm{M}} = \sum_{i=1}^{n} \left\{ \frac{q_i}{\sqrt{1 + r_i^2 d^2 + 2\vec{r}_i \cdot \vec{d}}} \right\}, \quad \vec{d} = \frac{\vec{r}}{r^2}, \quad d = \left|\vec{d}\right|.$$

If we choose d_x, d_y, and d_z, the components of $\vec{d}$, as DA variables, $\overline{\phi}_{\mathrm{M}}$ can be expressed as a DA vector, which can be considered as the Taylor expansion of $\overline{\phi}_{\mathrm{M}}$ with respect to d_x, d_y, and d_z at infinity. If we calculate the DA vector up to order p, the error of approximating ϕ by its expansion can be estimated as

$$|\epsilon| \leq C \cdot \left(\frac{a}{r}\right)^{p+1} \cdot \frac{1}{r-a}, \quad \text{with} \quad C = \sum_{i=1}^{n} |q_i|. \tag{2}$$

2.2 The Translation of the Far Multipole Expansion

The potential ϕ at $\vec{r}\,(x, y, z)$ of a far multipole expansion at the origin $\vec{O}\,(0, 0, 0)$ can be translated into another far multipole expansion at the point $\vec{r}\,'_o\left(x'_o, y'_o, z'_o\right)$. The new DA variables can be chosen as

$$\vec{d}\,' = \frac{\vec{r} - \vec{r}\,'_o}{r'^2} = \frac{\vec{r}\,'}{r'^2}.$$

With some direct algebra, one can find the relation between the new DA variables $\vec{d}\,'$ and the old DA variables $\vec{d}$ as

$$\vec{d} = \left(\vec{d}\,' + d'^2 \cdot \vec{r}\,'_o\right) \cdot R, \tag{3}$$

with $R = 1/\left(1 + r'^2{}_o d'^2 + 2\vec{r}\,'_o \cdot \vec{d}\,'\right)$. Eq. (3) can be considered the map between the new DA variables and the old DA variables, which we refer to as M_1. If we translate $\overline{\phi}_{\mathrm{M}}$ in the old frame into $\widetilde{\phi}_{\mathrm{M}}$ in the new frame by

$$\widetilde{\phi}_{\mathrm{M}} = \overline{\phi}_{\mathrm{M}} \circ M_1,$$

the potential in the new frame can be written as

$$\phi' = \widetilde{\phi}_{\mathrm{M}} \cdot d' \cdot \sqrt{R} = d' \cdot \overline{\phi}'_{\mathrm{M}}, \tag{4}$$

knowing that d in the old frame can be translated into the new frame as $d = d' \cdot \sqrt{R}$. The error of the DA expression for ϕ' has the same expression with Eq. (2) with r and a defined in the new frame.

2.3 The Local Expansion from the Charges

Consider an observer point $\vec{r}\ (x, y, z)$ within a spherical region of the radius b centered at $\vec{r}'_o(x'_o, y'_o, z'_o)$, then the electrostatic potential on the observer from n particles outside the spherical region can be expressed as a local expansion at $\vec{r}'_o(x'_o, y'_o, z'_o)$. We choose the DA variables as

$$\vec{d}' = \vec{r} - \vec{r}'_o = \vec{r}'. \tag{5}$$

Assuming the ith source particle has charge q_i and located at $\vec{r_i}\ (x_i, y_i, z_i)$, the local expansion of the potential is

$$\phi_{\mathrm{L}} = \sum_{i=1}^{n} \frac{q_i}{\left|\vec{r} - \vec{r_i}\right|} = \sum_{i=1}^{n} \frac{q_i}{\left|\vec{r}'_o - \vec{r_i} + \vec{d}'\right|}. \tag{6}$$

The error of the DA expression of ϕ_{L} up to order p can be estimated as

$$|\epsilon| \le C \cdot \left(\frac{r'}{b}\right)^{p+1} \cdot \frac{1}{b - r'} \quad \text{with} \quad C = \sum_{i=1}^{n} |q_i|. \tag{7}$$

2.4 The Conversion of the Far Multipole Expansion into a Local Expansion

Given a far multipole expansion at the origin $\vec{O}\ (0,0,0)$, a local expansion at $\vec{r}'_o(x'_o, y'_o, z'_o)$, which creates the same potential on the observers, can be found. It is called *local* because $\vec{r}'_o(x'_o, y'_o, z'_o)$ is close to the observer $\vec{r}\ (x, y, z)$. So it is natural to choose the new DA variables as

$$\vec{d}' = \vec{r} - \vec{r}'_o = \vec{r}' \tag{8}$$

where $\vec{r}'(x', y', z')$ are the new coordinates of the observer $\vec{r}\ (x, y, z)$ if we shift the origin to $\vec{r}'_o(x'_o, y'_o, z'_o)$. The old and the new DA variables have the relation

$$\vec{d} = \frac{\vec{r}}{r^2} = \left(\vec{r}'_o + \vec{d}'\right) \cdot R, \tag{9}$$

where $R = 1/\left|\vec{r}'_o + \vec{d}'\right|^2$. We note Eq. (9) as M_2. To convert the far multipole expansion in Eq. (4) into a local expansion, we need to work on the two parts separately. The $\overline{\phi'}_{\mathrm{M}}$ can be converted into $\widetilde{\phi}_{\mathrm{L}}$ in the new frame as

$$\widetilde{\phi}_{\mathrm{L}} = \overline{\phi'}_{\mathrm{M}} \circ M_2,$$

and d' can be converted into $\sqrt{R}$ in the new frame. Therefore, we have the local expansion as

$$\phi_{\mathrm{L}} = \widetilde{\phi}_{\mathrm{M}} \cdot \sqrt{R}. \tag{10}$$

Note that by now we obtained the expansion of the potential, not just a component of it, as a DA vector. The error of a local expansion up to order p converted from a far multipole expansion is

$$|\epsilon| \leq C \cdot \left(\frac{a}{r'_o}\right)^{p+1} \cdot \frac{1}{r'_o - a} + C \cdot \left(\frac{r'}{b}\right)^{p+1} \cdot \frac{1}{b - r'}, \tag{11}$$

where a, b, and C have the same meaning as in Eqs. (2) and (7).

2.5 The Translation of the Local Expansion

A local expansion at the origin $\vec{O}(0, 0, 0)$ can be translated to $\vec{r}'_o(x'_o, y'_o, z'_o)$, assuming that both points are close to the observer $\vec{r}\,(x, y, z)$. Choosing the new DA variable as the same as Eq. (5), the relation between the old and the new DA variables is just a linear shift:

$$\vec{d} = \vec{r}'_o + \vec{d}'. \tag{12}$$

We call Eq. (12) the map M_3, and then the new local expansion can be calculated by

$$\phi'_{\mathrm{L}} = \phi_{\mathrm{L}} \circ M_3. \tag{13}$$

This linear translation does not bring any additional error.

2.6 The Calculation of the Potential and the Field from the Expansions

It is straightforward to calculate the potential from a local expansion or a multipole expansion. Since we have the potential expressed as a pth order polynomial, we only need to plug in the value of (d_x, d_y, d_z) for each particle to obtain the potential for it.

The local expansion of the potential is a polynomial of the observer's coordinates. Taking the derivative of the potential with respect to a coordinate, one can obtain the $(p-1)$th-order polynomial for the field on the respective direction.

The DA variables in the multipole expansions are analytical functions of the coordinates. To calculate the field by the multipole expansion, we take the derivative with respect to the coordinates by the chain rule, and we obtain the expression of the field as

$$
\begin{aligned}
E_x &= \left\{ -\frac{\partial \overline{\phi}}{\partial d_x} \cdot \left(d^2 - 2d_x^2\right) + 2\frac{\partial \overline{\phi}}{\partial d_y} \cdot d_x d_y + 2\frac{\partial \overline{\phi}}{\partial d_z} \cdot d_x d_z + \overline{\phi} \cdot d_x \right\} \cdot d, \\
E_y &= \left\{ 2\frac{\partial \overline{\phi}}{\partial d_x} \cdot d_y d_x - \frac{\partial \overline{\phi}}{\partial d_y} \cdot \left(d^2 - 2d_y^2\right) + 2\frac{\partial \overline{\phi}}{\partial d_z} \cdot d_y d_z + \overline{\phi} \cdot d_y \right\} \cdot d, \\
E_z &= \left\{ 2\frac{\partial \overline{\phi}}{\partial d_x} \cdot d_z d_x + 2\frac{\partial \overline{\phi}}{\partial d_y} \cdot d_z d_y - \frac{\partial \overline{\phi}}{\partial d_z} \cdot \left(d^2 - 2d_z^2\right) + \overline{\phi} \cdot d_z \right\} \cdot d.
\end{aligned}
\tag{14}
$$

3. RESULTS OF NUMERICAL EXPERIMENTS

We now present some results of numerical experiments. In Figure 1, we compare the DA-based MLFMA with direct calculation using the Coulomb formula. The computational expense as a function of particles can be fitted by a straight line in a logarithmic representation for both cases. The slope for the direct Coulomb formula calculation is 2, reflecting the fact that for n charged particles, the computation time is proportional to n^2. The slope of the DA-based MLFMA is 1.073, which is very close to linear scaling with a slope of 1. Also, we can see that when $n > 1000$, the DA-based MLFMA outperforms the Coulomb formula in speed. Here, the DA-based MLFMA is conducted with DA in the fifth-order, while having a relative error less than 0.001.

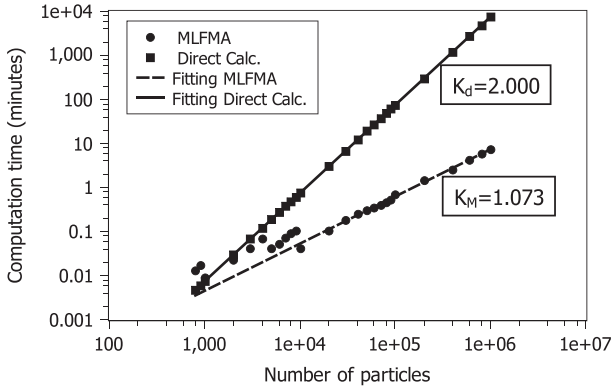

Figure 1 Efficiency of the DA-based MLFMA versus the Coulomb formula.

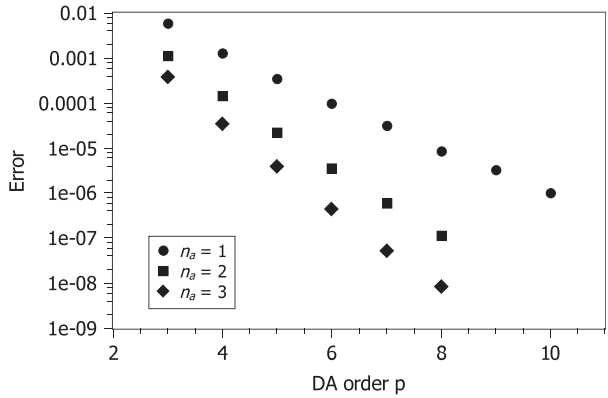

Figure 2 Error decreases as p and n_a increase (Zhang, 2013).

There are two ways to increase the accuracy. One is to increase the order of the DA calculations. The other is to increase the distance between two boxes whose interaction can be represented by expansions. As defined previously, expansions are used to represent the contribution of box A to the field in box B, when their distance is equal to or larger than the side length of A. To increase the accuracy, one can increase the distance to n_a times the side length of A, with $n_a \geq 1$. As shown in Figure 2, when p, the order of DA, increases, the error decreases. And for the same p, when n_a increases, the error decreases. We also notice that for a larger n_a, the error decreases faster (larger slope) with the increase of p. If one wants to calculate the field with a very high precision, it is better to increase n_a as well rather than merely increasing the DA order.

4. SPACE CHARGE SIMULATIONS OF PHOTOEMISSION AND COMPARISON WITH EXPERIMENTAL MEASUREMENTS

We have performed experiments to measure the ultrafast electron pulse dynamics immediately following photoemission (Tao et al., 2012) using a point projection imaging technique (Raman et al., 2009). A 50-fs laser pulse is applied to the gold photo cathode surface with an incidence of 45 deg to trigger the photoemission. The laser has a Gaussian profile with an elliptical cross section having $\sigma_x = 115$ μm and $\sigma_y = 81$ μm, which would generate a pancake-shaped electron bunch. A constant longitudinal extracting field perpendicular to the cathode surface is also applied. In simulations, instead of assuming an initial distribution, we generate the electrons

by groups following the three-step model (Jensen et al., 2010). The number of electrons in each group is in proportion to the laser pulse strength at the respective time slot. Once generated, the electrons move under the influence of the extraction field, the space charge field and the field of the image charge on the surface. The space charge field is calculated by the DA-based MLFMA. Based on COSY's MPI support, a parallel version of the algorithm is developed that allows the use of millions of macroparticles in our simulations.

The number of surviving electrons depends on the total amount of electrons generated and the strength of the extracting field. In Figure 3, we plot

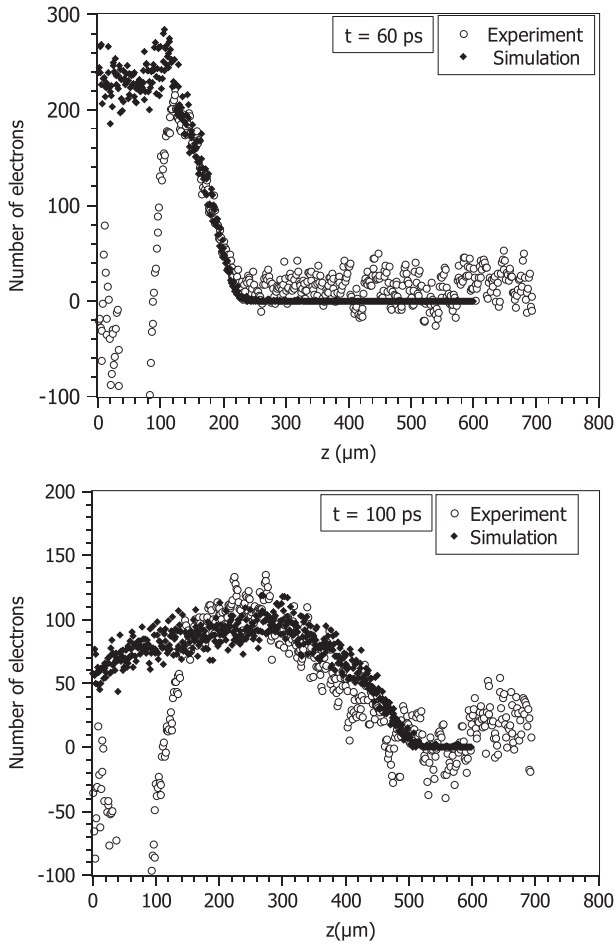

Figure 3 Longitudinal charge distribution of the electron bunch.

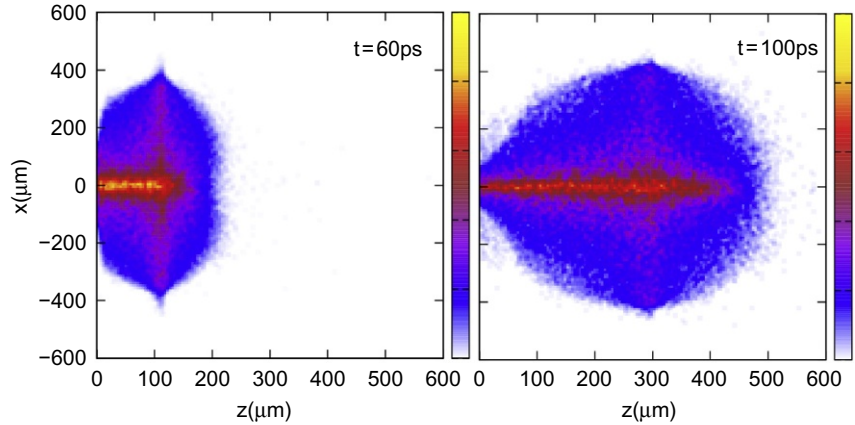

Figure 4 Charge distribution in *x-z* phase space (Zhang, 2013).

the longitudinal distribution of surviving electrons at 60 ps and 100 ps. The cathode surface is on the plane of $z=0$, and the extracting field is in the z-direction. Ignoring the experimental data close to the surface, the simulation and the experiment agree well for the peak position and the bunch shape. Figure 4 shows the charge density on the x-z plane at 60 ps and 100 ps, with x representing any transverse direction. These figures show the microstructure of the bunch and help us to understand the microdynamics of the space charge effect in the photoemission process. More simulations and discussions on our photoemission experiments can be found in Portman et al. (2013, 2015).

5. CONCLUSION

We have developed the DA-based MLFMA, which allows the calculation of the electrostatic field of an ensemble of charged particles in any arbitrary distribution with an efficiency that scales linearly with the number of particles. A parallel code for distributed structure cluster machines is also developed. In practice, we can simulate millions of particles in a reasonable time, and we have successfully applied this algorithm in the simulation of the photoemission process. The simulation results agree well with the experiments and reveal some information that is difficult to measure directly in experiments.

ACKNOWLEDGMENTS

We thank Kyoko Makino, Alexander Wittig, and Kiseok Chang for valuable discussions. The work was supported by the U.S. Department of Energy under Grants No.

DE-FG02-08ER41546 and No. DE-FG02-06ER46309, by U.S. National Science Foundation under Grant No. NSF-DMR 1126343, and by a seed grant for the development of an RF-enabled ultrafast electron microscope from the MSU Foundation. This research used high-performance computational resources, supported by the U.S. Department of Energy, and at Michigan State University High Performance Computing Center.

REFERENCES

Berz, M. (1999), *Modern map methods in particle beam physics*, San Diego: Academic Press.

Berz, M., & Makino, K. (2013). *COSY INFINITY version 9.1 programmer's manual, Technical Report MSUHEP-101214-rev,* Department of Physics and Astronomy, Michigan State University, East Lansing, MI. See also http://cosyinfinity.org.

Carrier, J., Greengard, L., & Rokhlin, V. (1988). A fast adaptive multipole algorithm for particle simulations. *SIAM Journal on Scientific and Statistical Computing 9*, 669–686.

Jensen, K., O'Shea, P., Feldman, D., & Shaw, J. (2010). Emittance of a field emission electron source. *Journal of Applied Physics, 107*(1), 014903, 1–14. http://dx.doi.org/10.1063/1.3267288.

Portman, J., Zhang, H., Makino, K., Ruan, C.-Y., Berz, M., & Duxbury, P. M. (2015), Multiscale modeling of the ultrafast electron microscope: From the photocathode to the sample. In *Proceedings of the Conference on Femtosecond Electron Imaging and Spectroscopy, FEIS 2013*. 117–130.

Portman, J., Zhang, H., Tao, Z., Makino, K., Berz, M., Duxbury, P. M., & Ruan, C.-Y. (2013). Computational and experimental characterization of high-brightness beams for femtosecond electron imaging and spectroscopy. *Applied Physics Letters, 103*(25), 253115, 1–5.

Raman, R., Tao, Z., Han, T., & Ruan, C.-Y. (2009). Ultrafast imaging of photoelectron packets generated from graphite surface. *Applied Physics Letters, 95*(18), 181108, 1–3.

Tao, Z., Zhang, H., Duxbury, P. M., Berz, M., & Ruan, C.-Y. (2012). Space charge effects in ultrafast electron diffraction and imaging. *Journal of Applied Physics, 111*(4), 044316, 1–10.

Zhang, H. (2013). The fast multipole method in the differential algebra framework for the calculation of 3D space charge fields, Ph.D. thesis, Michigan State University, East Lansing.

Zhang, H., & Berz, M. (2011). The fast multipole method in the differential algebra framework. *Nuclear Instruments and Methods A 645*, 338–344.